University of Baghdad
College of Engineering
JOURNAL OF ENGINEERING

Journal of Engineering
journal homepage: www.joe.uobaghdad.edu.iq
Number 9 Volume 27 September 2021

Mechanical and Energy Engineering

Thermal Buckling of Laminated Composite Plates Using a Simple Four Variable Plate Theory

Hussein Tawfeeq Yahea *
MSc student
College of Engineering
University of Baghdad
Mechanical Eng. Dept.
H.ALkhafaji1803M@coeng.uobaghdad.edu.iq

Widad Ibraheem Majeed
Asst.Prof Dr
College of Engineering
University of Baghdad
Mechanical Eng. Dept.
wedad.ibrahim@coeng.uobaghdad.edu.iq

ABSTRACT

In this study, the thermal buckling behavior of composite laminate plates cross-ply and angle-ply all edged simply supported subjected to a uniform temperature field is investigated, using a simple trigonometric shear deformation theory. Four unknown variables are involved in the theory, and satisfied the zero traction boundary condition on the surface without using shear correction factors, Hamilton's principle is used to derive equations of motion depending on a Simple Four Variable Plate Theory for cross-ply and angle-ply, and then solved through Navier's double trigonometric sequence, to obtain critical buckling temperature for laminated composite plates. Effect of changing some design parameters such as, orthotropy ratio (E1/E2), aspect ratio (a/b), thickness ratio (a/h), thermal expansion coefficient ratio (α2/α1), are investigated, which have the same behavior and good agreement when compared with previously published results with maximum discrepancy (0.5%).

Keywords: Thermal buckling, shear deformation, cross-ply and angle-ply.

الاستقرار الحراري لصفائح الألواح المركبة باستخدام نظرية الصفائح ذات الاربع متغيرات البسيط

*** حسين توفيق يحيى**
طالب ماجستير
جامعة بغداد – كلية الهندسة – قسم الهندسة الميكيانيكية

وداد ابراهيم مجيد
استاذ مساعد
جامعة بغداد – كلية الهندسة – قسم الهندسة الميكيانيكية

الخلاصة

في هذه الدراسة ، تم التحقيق في سلوك الالتواء الحراري لألواح الرقائق المركبة ذات الطبقات المتقاطعة والزاوية ذات الحواف المدعمة ببساطة والتي تخضع لحقل درجة حرارة موحد ، وذلك باستخدام نظرية تشوه القص المثلثية البسيطة ، وتشارك أربعة متغيرات غير معروفة في النظرية ، استيفاء شرط حدود الجر الصفري على السطح دون استخدام عوامل تصحيح القص ، وتعتمد معادلات الحركة على نظرية الألواح المتغيرة الأربعة البسيطة والزاوية المتقاطعة ، ويستخدم مبدأ هاملتون لاشتقاق المعادلات الحاكمة ، ثم يتم حلها من خلال مثلث نافير المزدوج. التسلسل ، للحصول على درجة حرارة الالتواء الحرجة للألواح

*Corresponding author
Peer review under the responsibility of University of Baghdad.
https://doi.org/10.31026/j.eng.2021.09.01

Article received: 14/ 4/2021
Article accepted: 15/6/2021
Article published:1/9/2021

المركبة المصفحة. خلال هذا البحث ، تم عرض تأثير معلمات التصميم ، نسبة (E1 / E2) ، نسبة العرض إلى الارتفاع (a / b) ، نسبة السماكة (a / h) ، نسبة معامل التمدد الحراري (α1 / α2). يمكن الاستنتاج أن هذه النظرية تعطي نفس التصرف وتوافق جيد عند مقارنتها بالنتائج المنشورة سابقًا مع أقصى قدر من اختلاف (0.5٪).

1. INTRODUCTION

Thermal buckling research is critical for structural components used in high-speed aircraft, rockets, and space vehicles, where thermal loads are caused by aerodynamic and solar radiation heating, as well as for nuclear reactors and chemical planets, which are typically subjected to an elevated temperature regime during their service lives, **(Cetkovic, 2016), (Shen, 2013),** concerned thermal buckling and post-buckling behavior which presented for fiber-reinforced laminated plates subjected to in-plane temperature variation and resting on an elastic foundation, The governing equations are based on a higher order shear deformation plate theory that includes plate–foundation interaction and the thermal effect **(Mansouri and Shariyat, 2014).** The related differential equations governing the system are solved using a novel differential quadrature process (DQM). Although the refined four parameters plate theory (RPT) needs less displacement parameters and is usually more accurate than the pth order generalization of theory of Reddy (GRT), both are less accurate than the third order five parameters of Reddy theory (TOST). **(Shaterzadeh, Abolghasemi and Rezaei, 2014)** studied thermal buckling analysis of symmetric and antisymmetric laminated composite plates with a cut-out, subjected to a uniform temperature rise for different boundary conditions, The stiffness matrices and thermal force vector are derived according to first-order shear deformation theory (FSDT)**. (Ounis, Tati and Benchabane, 2014)** focused on the classical plate theory, and investigated the thermal buckling behavior of composite laminated plates under uniform temperature distribution. The present finite element is a combination of a linear isoparametric membrane element and a high precision rectangular Hermitian element**. (Vosoughi and Nikoo, 2015)** developed a hybrid method for maximizing fundamental natural frequency and thermal buckling temperature of laminated composite plates that is a new combination of the differential quadrature method (DQM) based on the first-order shear deformation theory (FSDT) of plates and are discretized using the (DQM). **(Jin *et al.*, 2015)** used of the Digital Image Correlation (DIC) technique to investigate the thermal buckling of a circular laminated composite plate subjected to a uniform distribution of temperature load, the results of the buckling temperature from DIC were close to the theoretical buckling temperature of the circular plate found using a simply supported boundary condition **(Cetkovic, 2016).** Thermal buckling of laminated composite plates was investigated using Reddy's Layerwise theory and a new version of Reddy's Layer-wise Theory. The strong form is used to derive Navier's analytical solution, while the weak form is discretized using the isoparametric finite element approximation. **(Hussein and Alasadi, 2018)** used two methods to study the stress analysis of composite plates subjected to the uniform temperature at various factors. The first method is an experimental test by using a dial gauge, and the second method is based on a finite element solution using a computer program resulted in the thermal strain increases with increasing temperature difference (ΔT) and decreased with increasing the fiber volume fraction (Vf). **(Xing and Wang, 2017)** investigated the critical buckling temperature of functionally graded rectangular thin plates. closed form solutions for the critical thermal parameter are obtained for the plate with different

boundary conditions under uniform, linear and nonlinear temperature fields using the separation-of-variable method. **(Vescovini *et al.*, 2017)** used Ritz-based variable kinematic formulation to research thermal buckling of composite plates and sandwich panels. They represented arbitrary groups of plies composing the panel. Critical temperatures obtained were for, with and without accounting for the pre-buckling. **(Tran, Wahab, and Kim, 2017)** developed a six-variable quasi-3D model with one additional variable in the transverse displacement of higher-order shear deformation theory (HSDT), resulting in a temperature rise in a plate structure that produces non-zero transverse normal strain. The governing equation is discretized by isogeometric analysis (IGA). **(Manickam *et al.*, 2018)** used a finite element approach based on first-order shear deformation theory, investigated the thermal buckling behavior of variable stiffness laminated composite plates subjected to thermal loads. The developed governing equations are solved using an eigenvalue method, in accordance with the concept of minimizing total potential energy. **(Sadiq and Majeed, 2019)** using a higher-order displacement field, Mantari et al. determined the critical buckling temperature of an angle-ply laminated plate. This displacement field is based on a constant "m" chosen to generate results consistent with three-dimensional elasticity (3-D) theory. The equations of motion for simply assisted laminated plates based on higher-order theory were deduced and solved using Hamilton's principle. **(Kiani, 2020)** studied thermal buckling nature of composite laminated skew plates reinforced by graphene platelets. The formulation is based on the first-order shear deformation plate theory. It is presumed that each layer of the composite laminated plate can have different volume fraction of graphene platelets leading to a through-the-thickness piecewise functionally graded medium. The thermal buckling behavior of various shapes of functionally graded carbon nanotube reinforced composite (FG-CNTRC) plates is investigated by **(Torabi, Ansari and Hassani, 2019)** using higher-order shear deformation plate theory. Using Hamilton's principle, discretized equations of motion are finally obtained. A wide range of numerical results is also presented to analyze the thermal buckling behavior of various shapes of FG-CNTRC plates. **(Do and Lee, 2019)** used a mesh-free approach to describe the buckling behavior of multilayered composite plates in thermal environments, including a functionally graded material (FGM) layer. Thermal buckling of a composite plate laminated with an FGM layer is modeled using an improved Moving Kriging (MK) meshless approach based on n^{th}-order shear deformation theory. **(Tocci Monaco *et al.*, 2020)** used second-order strain gradient theory, and investigated the vibrations and buckling of thin laminated composite nanoplates in a humid-thermal setting. Hamilton's theorem is used to solve equations of motion. To amass analytical data the Navier displacement area was considered for both cross-ply and angle-ply laminates, and the findings revealed a wide range of angle-ply cases that are not often encountered in the published literature**. (Yang *et al.*, 2020)** examined the effect of geometrical nonlinearities associated with pressure loads on the thermal buckling and dynamic properties of composite plates. Thermal buckling and modal analysis was performed on a four-sided simply supported rectangular composite plate subjected to a variety of pressure fields. The numerical results indicate that as the pressure increases, both the mode frequencies and critical buckling temperature of the plate increase. The thermal buckling behavior of a composite plate structure with a number of nano fractions was investigated by **(Al-Waily, Al-Shammari and Jweeg, 2020)** using analytical and

numerical methods. The general motion equation for thermal buckling load was derived and the results were compared to the numerical results. **(Alabas and Majid, 2020)** and based on classical laminated plate theory, used the improved Rayleigh-Ritz method and Fourier series to evaluate the thermal buckling behavior of laminated composite thin plates with a general elastic boundary condition applied to an in-plane uniform temperature distribution (CLPT).

In the present work, the efficiency of a four-variable refined trigonometric shear deformation theory for thermal buckling analysis of cross-ply and angle-ply laminated composite plates is investigated. The theory does not require a problem-dependent shear correction factor. Finally, the numerical results obtained using the present theory are compared to those obtained using other theories and show a high degree of agreement.

2. DISPLACEMENT FIELD AND STRAIN

2.1Displacement field

The displacement field associated with present theory is, **(Sayyad, Shinde and Ghugal, 2016)** :

$$u(x,y,z,t) = u_0(x,y,t) - z\frac{\partial w_b(x,y,t)}{\partial x} - \left(z - \frac{h}{\pi}\sin\frac{\pi z}{h}\right)\frac{\partial w_s(x,y,t)}{\partial x}$$

$$v(x,y,z,t) = v_0(x,y,t) - z\frac{\partial w_b(x,y,t)}{\partial x} - \left(z - \frac{h}{\pi}\sin\frac{\pi z}{h}\right)\frac{\partial w_s(x,y,t)}{\partial x} \quad (1)$$

$$w(x,y,t) = w_b(x,y,t) + w_s(x,y,t)$$

Where (u_0, v_0, w_b, w_s) are the Four unknown displacements

2.2The linear strain-displacement relation is (Reddy, 2003):-

$$\varepsilon_x = \frac{\partial u}{\partial x}, \quad \varepsilon_y = \frac{\partial v}{\partial y}, \quad \varepsilon_z = \frac{\partial w}{\partial z}, \quad \gamma_{xy} = 2\varepsilon_{xy} = \frac{\partial u}{\partial y} + \frac{\partial v}{\partial x}$$

$$\gamma_{xz} = 2\varepsilon_{xz} = \frac{\partial u}{\partial z} + \frac{\partial w}{\partial x} \quad (2)$$

$$\gamma_{yz} = 2\varepsilon_{yz} = \frac{\partial v}{\partial z} + \frac{\partial w}{\partial y}$$

Substituting Eqs (1) in Eqs (2):

$$\begin{Bmatrix}\varepsilon_x\\ \varepsilon_y\\ \gamma_{xy}\end{Bmatrix} = \begin{Bmatrix}\varepsilon_x^0\\ \varepsilon_y^0\\ \gamma_{xy}^0\end{Bmatrix} + Z\begin{Bmatrix}\varepsilon_x^b\\ \varepsilon_y^b\\ \gamma_{xy}^b\end{Bmatrix} + f(z)\begin{Bmatrix}\varepsilon_x^s\\ \varepsilon_y^s\\ \gamma_{xy}^s\end{Bmatrix} \quad and \quad \begin{Bmatrix}\gamma_{yz}\\ \gamma_{xz}\end{Bmatrix} = g(z)\begin{Bmatrix}\gamma_{yz}^s\\ \gamma_{xz}^s\end{Bmatrix} \quad (3)$$

Then:

$$\begin{Bmatrix}\varepsilon_x\\ \varepsilon_y\\ \gamma_{xy}\end{Bmatrix}=\begin{Bmatrix}\frac{\partial u}{\partial x}\\ \frac{\partial v}{\partial y}\\ \frac{\partial u}{\partial y}+\frac{\partial v}{\partial x}\end{Bmatrix}=\begin{Bmatrix}\frac{\partial u_0}{\partial x}\\ \frac{\partial v_0}{\partial y}\\ \frac{\partial u_0}{\partial y}+\frac{\partial v_0}{\partial x}\end{Bmatrix}-Z\begin{Bmatrix}\frac{\partial^2 w_b}{\partial x^2}\\ \frac{\partial^2 w_b}{\partial y^2}\\ 2\frac{\partial^2 w_b}{\partial x\partial y}\end{Bmatrix}-f(z)\begin{Bmatrix}\frac{\partial^2 w_s}{\partial x^2}\\ \frac{\partial^2 w_s}{\partial y^2}\\ 2\frac{\partial^2 w_s}{\partial x\partial y}\end{Bmatrix}$$

$$\begin{Bmatrix}\gamma_{yz}\\ \gamma_{xz}\end{Bmatrix}=\begin{Bmatrix}\frac{\partial v}{\partial z}+\frac{\partial w}{\partial y}\\ \frac{\partial u}{\partial z}+\frac{\partial w}{\partial x}\end{Bmatrix}=\cos\frac{\pi z}{h}\begin{Bmatrix}\frac{\partial w_s}{\partial y}\\ \frac{\partial w_s}{\partial x}\end{Bmatrix},\quad \varepsilon_z=0, \tag{4}$$

Where $f(z)=z-\frac{h}{\pi}\sin\frac{\pi z}{h}\quad and\quad g(z)=\cos\frac{\pi z}{h}$

3. VIRTUAL WORK PRINCIPLE

$$0=\int_0^T(\delta U+\delta V)dt \tag{5}$$

Where (δU) is Virtual strain energy and (δV) is Virtual external work done are given, **(Reddy, 2003)**, the Virtual strain energy (δU) is:

$$\delta U=\int_0^b\int_0^a\int_{\frac{-h}{2}}^{\frac{h}{2}}\left[\sigma_x\ \delta\varepsilon_x+\sigma_y\ \delta\varepsilon_y+\sigma_{xy}\ \delta\gamma_{xy}+\sigma_{yz}\ \delta\gamma_{yz}+\sigma_{xz}\ \delta\gamma_{xz}\right]dzdxdy \tag{6}$$

Where $\delta\varepsilon=\delta\varepsilon^0+z\delta\varepsilon^b+f(z)\delta\varepsilon^s$ in general

$$\begin{Bmatrix}N_x\\ N_y\\ N_{xy}\end{Bmatrix}=\sum_{k=1}^N\int_{\frac{h}{2}}^{\frac{h}{2}}\begin{Bmatrix}\sigma_x\\ \sigma_y\\ \tau_{xy}\end{Bmatrix}dz\ ,\quad \begin{Bmatrix}M_x^b\\ M_y^b\\ M_{xy}^b\end{Bmatrix}=\sum_{k=1}^N\int_{\frac{h}{2}}^{\frac{h}{2}}\begin{Bmatrix}\sigma_x\\ \sigma_y\\ \tau_{xy}\end{Bmatrix}z\,dz\ ,$$

$$\begin{Bmatrix}M_x^s\\ M_y^s\\ M_{xy}^s\end{Bmatrix}=\sum_{k=1}^N\int_{\frac{h}{2}}^{\frac{h}{2}}\begin{Bmatrix}\sigma_x\\ \sigma_y\\ \tau_{xy}\end{Bmatrix}f(z)\,dz\ ,\begin{Bmatrix}Q_x\\ Q_y\end{Bmatrix}=\sum_{k=1}^N\int_{\frac{h}{2}}^{\frac{h}{2}}\begin{Bmatrix}\tau_{xz}\\ \tau_{yz}\end{Bmatrix}g(z)dz \tag{7}$$

Substituting Eqs (7) in Eqs (6):

$$\delta U=\int_0^b\int_0^a\Big[N_x\frac{\partial\delta u_0}{\partial x}-M_x^b\frac{\partial^2\delta w_b}{\partial x^2}-M_x^s\frac{\partial^2\delta w_s}{\partial x^2}+N_y\frac{\partial\delta v_0}{\partial y}-M_y^b\frac{\partial^2\delta w_b}{\partial y^2}-M_y^s\frac{\partial^2\delta w_s}{\partial y^2}+\quad N_{xy}\Big(\frac{\partial\delta u_0}{\partial y}+\frac{\partial\delta v_0}{\partial x}\Big)-2M_{xy}^b\frac{\partial^2\delta w_b}{\partial x\partial y}-2M_{xy}^s\frac{\partial^2\delta w_s}{\partial x\partial y}+Q_x\frac{\partial\delta w_s}{\partial x}+Q_y\frac{\partial\delta w_s}{\partial y}\Big]dxdy \tag{8}$$

Now using integration by parts, the form for Virtual strain energy (δU) is found:

$$\delta U = \int_0^b \int_0^a \left[\left(\frac{-\partial N_x}{\partial x} - \frac{\partial N_{xy}}{\partial y} \right) \delta u_0 + \left(\frac{-\partial N_y}{\partial y} - \frac{\partial N_{xy}}{\partial x} \right) \delta v_0 + \left(\frac{-\partial^2 M_x^b}{\partial x^2} - \frac{\partial^2 M_y^b}{\partial y^2} - \frac{2\partial^2 M_{xy}^b}{\partial x \partial y} \right) \delta w_b \right.$$
$$+ \left(\frac{-\partial^2 M_x^s}{\partial x^2} - \frac{\partial^2 M_y^s}{\partial y^2} - \frac{2\partial^2 M_{xy}^s}{\partial x \partial y} - \frac{\partial Q_x}{\partial x} - \frac{\partial Q_y}{\partial y} \right) \delta w_s \Big] dxdy$$
$$+ \oint \left[(N_x + N_y) \partial u_0 + (N_y + N_{xy}) \partial v_0 + \left(\frac{\partial M_x^b}{\partial x} + \frac{\partial M_y^b}{\partial y} - \frac{2\partial M_{xy}^b}{\partial x} \right) \delta w_b \right.$$
$$+ \left(\frac{\partial M_x^s}{\partial x} + \frac{\partial M_y^s}{\partial y} + \frac{2\partial M_{xy}^s}{\partial x} + Q_x + Q_y \right) \delta w_s + \left(-M_y^b - 2M_{xy}^b \right) \frac{\partial \delta w_b}{\partial y}$$
$$+ \left(-M_y^s - 2M_{xy}^s \right) \frac{\partial \delta w_s}{\partial y} - M_x^b \frac{\partial \delta w_b}{\partial x} - M_x^s \frac{\partial \delta w_s}{\partial x} \Big] ds \quad (9)$$

While the Virtual external work done by thermal applied load (δV) is :

$$\delta V = -\frac{1}{2} \int_0^b \int_0^a \left[N_x^T \delta \left(\frac{\partial w}{\partial x} \right)^2 + N_y^T \delta \left(\frac{\partial w}{\partial y} \right)^2 + N_{xy}^T \delta \left(\frac{\partial w}{\partial x} \frac{\partial w}{\partial y} \right) \right] dxdy \quad (10)$$

$$\delta V = -\frac{1}{2} \int_0^b \int_0^a \left[2N_x^T \frac{\partial w}{\partial x} \frac{\partial \delta w}{\partial x} + 2N_y^T \frac{\partial w}{\partial y} \frac{\partial \delta w}{\partial y} + N_{xy}^T \left(\frac{\partial w}{\partial x} \frac{\partial \delta w}{\partial y} + \frac{\partial w}{\partial y} \frac{\partial \delta w}{\partial x} \right) \right] dxdy \quad (11)$$

Where $\mathrm{w} = \mathrm{w_b} + \mathrm{w_s}$ (assumption)

When integrating by parts Eq (11) and using divergence theory:

$$\delta \mathrm{V} = -\int_0^{\mathrm{b}} \int_0^{\mathrm{a}} \left(\mathrm{N_x^T} \frac{\partial^2 (\mathrm{w_b} + \mathrm{w_s})}{\partial \mathrm{x}^2} + \mathrm{N_y^T} \frac{\partial^2 (\mathrm{w_b} + \mathrm{w_s})}{\partial \mathrm{y}^2} + 2\mathrm{N_{xy}^T} \frac{\partial^2 (\mathrm{w_b} + \mathrm{w_s})}{\partial \mathrm{x}\, \partial \mathrm{y}} \right) (\delta \mathrm{w_b} + \delta \mathrm{w_s}) \mathrm{dxdy} -$$
$$\oint \left(\mathrm{N_x^T} \frac{\partial (\mathrm{w_b} + \mathrm{w_s})}{\partial x} + \mathrm{N_y^T} \frac{\partial (\mathrm{w_b} + \mathrm{w_s})}{\partial y} + \mathrm{N_{xy}^T} \frac{\partial (\mathrm{w_b} + \mathrm{w_s})}{\partial \mathrm{y}} nx + \mathrm{N_{xy}^T} \frac{\partial (\mathrm{w_b} + \mathrm{w_s})}{\partial \mathrm{x}} ny \right) (\delta \mathrm{w_b} + \delta \mathrm{w_s})\, ds \quad (12)$$

where

$$\begin{Bmatrix} \mathrm{N_x^T} \\ \mathrm{N_y^T} \\ \mathrm{N_{xy}^T} \end{Bmatrix} = \sum_{K=1}^{N} \int_{\frac{-h}{2}}^{\frac{h}{2}} \begin{bmatrix} Q_{11} & Q_{12} & Q_{16} \\ Q_{12} & Q_{22} & Q_{26} \\ Q_{16} & Q_{26} & Q_{66} \end{bmatrix} \begin{Bmatrix} \alpha_{xx} \\ \alpha_{yy} \\ \alpha_{xy} \end{Bmatrix} \Delta T cr\, dz \quad (13)$$

$$[A_{ij}] = \int_{\frac{-h}{2}}^{\frac{h}{2}} [Q_{ij}] \{\alpha_{ij}\} dz \ , \ \ i,j = (1,2,6) \quad (14)$$

Now substituting for δU *and* δV, from Eqs (9),(12) in Eq (5):

$$0 = \int_0^t \left\{ \int_0^b \int_0^a \left[\left(\frac{-\partial N_x}{\partial x} - \frac{\partial N_{xy}}{\partial y} \right) \delta u_0 + \left(\frac{-\partial N_y}{\partial y} - \frac{\partial N_{xy}}{\partial x} \right) \delta v_0 + \left(\frac{-\partial^2 M_x^b}{\partial x^2} - \frac{\partial^2 M_y^b}{\partial y^2} - \frac{2\partial^2 M_{xy}^b}{\partial x \partial y} \right) \delta w_b + \left(\frac{-\partial^2 M_x^s}{\partial x^2} - \frac{\partial^2 M_y^s}{\partial y^2} - \right. \right. \right.$$
$$\left. \left. \left. \frac{2\partial^2 M_{xy}^s}{\partial x \partial y} - \frac{\partial Q_x}{\partial x} - \frac{\partial Q_y}{\partial y} \right) \delta w_s - \left(\mathrm{N_x^T} \frac{\partial^2 (\mathrm{w_b} + \mathrm{w_s})}{\partial \mathrm{x}^2} + \mathrm{N_y^T} \frac{\partial^2 (\mathrm{w_b} + \mathrm{w_s})}{\partial \mathrm{y}^2} + 2\mathrm{N_{xy}^T} \frac{\partial^2 (\mathrm{w_b} + \mathrm{w_s})}{\partial \mathrm{x}\, \partial \mathrm{y}} \right) (\delta \mathrm{w_b} + \delta \mathrm{w_s}) + \right] dA +$$

$$\oint\left[\left(\left(N_x+N_y\right)\partial u_0+\left(N_y+N_{xy}\right)\partial v_0+\left(\frac{\partial M_x^b}{\partial x}+\frac{\partial M_y^b}{\partial y}-\frac{2\partial M_{xy}^b}{\partial x}\right)\delta w_b+\left(\frac{\partial M_x^s}{\partial x}+\frac{\partial M_y^s}{\partial y}+\frac{2\partial M_{xy}^s}{\partial x}+Q_x+Q_y\right)\delta w_s+\left(-M_y^b-2M_{xy}^b\right)\frac{\partial\delta w_b}{\partial y}+\left(-M_y^s-2M_{xy}^s\right)\frac{\partial\delta w_s}{\partial y}-M_x^b\frac{\partial\delta w_b}{\partial x}-M_x^s\frac{\partial\delta w_s}{\partial x}\right)-\left(\mathrm{N_x^T}\ \frac{\partial(\mathrm{w_b+w_s})}{\partial x}+\mathrm{N_y^T}\ \frac{\partial(\mathrm{w_b+w_s})}{\partial y}+\mathrm{N_{xy}^T}\ \frac{\partial(\mathrm{w_b+w_s})}{\partial \mathrm{y}}nx+\mathrm{N_{xy}^T}\ \frac{\partial(\mathrm{w_b+w_s})}{\partial \mathrm{x}}ny\right)(\delta \mathrm{w_b}+\delta \mathrm{w_s})\right]ds\Big\}dt \quad (15)$$

4. EQUATIONS OF MOTION

The Euler-Lagrange equations are obtained by setting coefficients $\left(\delta u_{0,}\delta v_{0,}\delta w_{b,}\delta w_s\right)$ over Area of Eq (15) to zero as follows **(Reddy, 2003):**

$$\delta u_0:\frac{\partial N_x}{\partial x}+\frac{\partial N_{xy}}{\partial y}=0 \quad (16)$$

$$\delta v_0:\frac{\partial N_{xy}}{\partial x}+\frac{\partial N_y}{\partial y}=0 \quad (17)$$

$$\delta w_b:\left(\frac{\partial^2 M_x^b}{\partial x^2}+\frac{\partial^2 M_y^b}{\partial y^2}+\frac{2\partial^2 M_{xy}^b}{\partial x\partial y}\right)+\left(\mathrm{N_x^T}\ \frac{\partial^2(\mathrm{w_b+w_s})}{\partial \mathrm{x}^2}+\mathrm{N_y^T}\ \frac{\partial^2(\mathrm{w_b+w_s})}{\partial \mathrm{y}^2}+2\mathrm{N_{xy}^T}\ \frac{\partial^2(\mathrm{w_b+w_s})}{\partial \mathrm{x}\,\partial \mathrm{y}}\right)=0 \quad (18)$$

$$\partial w_s:\left(\frac{\partial^2 M_x^s}{\partial x^2}+\frac{\partial^2 M_y^s}{\partial y^2}+\frac{2\partial^2 M_{xy}^s}{\partial x\partial y}+\frac{\partial Q_x}{\partial x}+\frac{\partial Q_y}{\partial y}\right)\left(\mathrm{N_x^T}\ \frac{\partial^2(\mathrm{w_b+w_s})}{\partial \mathrm{x}^2}+\mathrm{N_y^T}\ \frac{\partial^2(\mathrm{w_b+w_s})}{\partial \mathrm{y}^2}+\ 2\mathrm{N_{xy}^T}\ \frac{\partial^2(\mathrm{w_b+w_s})}{\partial \mathrm{x}\,\partial \mathrm{y}}\right)=0 \quad (19)$$

The stress - strain relations are(Reddy, 2003):-

$$\begin{Bmatrix}\sigma_x\\ \sigma_y\\ \tau_{xy}\end{Bmatrix}=\begin{bmatrix}\bar{Q}_{11} & \bar{Q}_{12} & \bar{Q}_{16}\\ \bar{Q}_{12} & \bar{Q}_{22} & \bar{Q}_{26}\\ \bar{Q}_{16} & \bar{Q}_{26} & \bar{Q}_{66}\end{bmatrix}\begin{Bmatrix}\varepsilon_x\\ \varepsilon_y\\ \gamma_{xy}\end{Bmatrix},\ and\ \begin{Bmatrix}\tau_{yz}\\ \tau_{xz}\end{Bmatrix}=\begin{bmatrix}\bar{Q}_{44} & \bar{Q}_{45}\\ \bar{Q}_{45} & \bar{Q}_{55}\end{bmatrix}\begin{Bmatrix}\gamma_{yz}\\ \gamma_{xz}\end{Bmatrix} \quad (20)$$

$$\text{let}\ \{A_{ij},B_{ij},AS_{ij},D_{ij}\}=\sum_{k=1}^{N}\bar{Q}_{ij}^k\int_{\frac{-h}{2}}^{\frac{h}{2}}\{1,z,f(z),z^2\}\,dz \qquad (i=j=1,2,6) \quad (21)$$

$$\{BS_{ij},ASS_{ij}\}=\sum_{k=1}^{N}\bar{Q}_{ij}^k\int_{\frac{-h}{2}}^{\frac{h}{2}}f(z)\{z,f(z)\}\,dz \qquad (i=j=1,2,6)$$

$$\text{And}\ \{ACC_{ij}\}=\sum_{k=1}^{N}\bar{Q}_{ij}^k\int_{\frac{-h}{2}}^{\frac{h}{2}}[g(z)]^2\,dz \qquad (\mathrm{i=j=4,5}) \quad (22)$$

Where $\{A_{ij},B_{ij},AS_{ij},D_{ij},BS_{ij},ASS_{ij},ACC_{ij}\}$ are the laminate stiffness coefficients

Substituting Eq (20) in Eqs (7) then Substituting Eqs (21)-(22) in the result equations obtain

$$\begin{Bmatrix} N_x \\ N_y \\ N_{xy} \\ M_x^b \\ M_y^b \\ M_{xy}^b \\ M_x^s \\ M_y^s \\ M_{xy}^s \end{Bmatrix} = \begin{bmatrix} A_{11} & A_{12} & A_{16} & B_{11} & B_{12} & B_{16} & AS_{11} & AS_{12} & AS_{16} \\ A_{12} & A_{22} & A_{26} & B_{12} & B_{22} & B_{26} & AS_{12} & AS_{22} & AS_{26} \\ A_{16} & A_{26} & A_{66} & B_{16} & B_{26} & B_{66} & AS_{16} & AS_{26} & AS_{66} \\ B_{11} & B_{12} & B_{16} & D_{11} & D_{12} & D_{16} & BS_{11} & BS_{12} & BS_{16} \\ B_{12} & B_{22} & B_{26} & D_{12} & D_{22} & D_{26} & BS_{12} & BS_{22} & BS_{26} \\ B_{16} & B_{26} & B_{66} & D_{16} & D_{26} & D_{66} & BS_{16} & BS_{26} & BS_{66} \\ AS_{11} & AS_{12} & AS_{16} & BS_{11} & BS_{12} & BS_{16} & ASS_{11} & ASS_{12} & ASS_{16} \\ AS_{12} & AS_{22} & AS_{26} & BS_{12} & BS_{22} & BS_{26} & ASS_{12} & ASS_{22} & ASS_{26} \\ AS_{16} & AS_{26} & AS_{66} & BS_{16} & BS_{26} & BS_{66} & ASS_{16} & ASS_{26} & ASS_{66} \end{bmatrix} \begin{Bmatrix} \varepsilon_x^0 \\ \varepsilon_y^0 \\ \gamma_{xy}^0 \\ \varepsilon_x^b \\ \varepsilon_y^b \\ \gamma_{xy}^b \\ \varepsilon_x^s \\ \varepsilon_y^s \\ \gamma_{xy}^s \end{Bmatrix}$$

$$\begin{Bmatrix} Q_y \\ Q_x \end{Bmatrix} = \begin{bmatrix} ACC_{44} & ACC_{45} \\ ACC_{45} & ACC_{55} \end{bmatrix} \begin{Bmatrix} \gamma_{yz} \\ \gamma_{xz} \end{Bmatrix} \quad (23)$$

Where $\{N_x; N_y; N_{xy}\}$ are the in-plane forces, while $\{M_x^b; M_y^b; M_{xy}^b\}$ are the moments, and $\{Q_x; Q_y\}$ are the transverse shear force but $\{M_x^s; M_y^s; M_{xy}^s\}$ are the moment resultants related with the transverse shear deformation **(Sayyad, Shinde and Ghugal, 2016)**, which are substituted from Eqs. (23) in terms of displacement variables in Eqs (21) – (24) , the governing equations of equilibrium will be:-

$$\delta u_0: -A_{11}\frac{\partial^2 u_0}{\partial x^2} - 2A_{16}\frac{\partial^2 u_0}{\partial x \partial y} - A_{66}\frac{\partial^2 u_0}{\partial y^2} - A_{16}\frac{\partial^2 v_0}{\partial x^2} - (A_{12}+A_{66})\frac{\partial^2 v_0}{\partial x \partial y} - A_{26}\frac{\partial^2 v_0}{\partial y^2} + B_{11}\frac{\partial^3 w_b}{\partial x^3} + (B_{12}+2B_{66})\frac{\partial^3 w_b}{\partial x \partial y^2} + 3B_{16}\frac{\partial^3 w_b}{\partial x^2 \partial y} + B_{26}\frac{\partial^3 w_b}{\partial y^3} + AS_{11}\frac{\partial^3 w_s}{\partial x^3} + (AS_{12}+2AS_{66})\frac{\partial^3 w_s}{\partial x \partial y^2} + 3AS_{16}\frac{\partial^3 w_s}{\partial x^2 \partial y} + AS_{26}\frac{\partial^3 w_s}{\partial y^3} = 0 \quad (24)$$

$$\delta v_0: -A_{16}\frac{\partial^2 u_0}{\partial x^2} - (A_{12}+A_{66})\frac{\partial^2 u_0}{\partial x \partial y} - A_{26}\frac{\partial^2 u_0}{\partial y^2} - A_{66}\frac{\partial^2 v_0}{\partial x^2} - 2A_{26}\frac{\partial^2 v_0}{\partial x \partial y} - A_{22}\frac{\partial^2 v_0}{\partial y^2} + B_{16}\frac{\partial^3 w_b}{\partial x^3} + 3B_{26}\frac{\partial^3 w_b}{\partial x \partial y^2} + (B_{12}+2B_{66})\frac{\partial^3 w_b}{\partial x^2 \partial y} + B_{22}\frac{\partial^3 w_b}{\partial y^3} + AS_{16}\frac{\partial^3 w_s}{\partial x^3} + 3AS_{26}\frac{\partial^3 w_s}{\partial x \partial y^2} + (AS_{12}+2AS_{66})\frac{\partial^3 w_s}{\partial x^2 \partial y} + AS_{22}\frac{\partial^3 w_s}{\partial y^3} = 0 \quad (25)$$

$$\delta w_b: -B_{11}\frac{\partial^3 u_0}{\partial x^3} - 3B_{16}\frac{\partial^3 u_0}{\partial x^2 \partial y} - (B_{12}+2B_{66})\frac{\partial^3 u_0}{\partial x \partial y^2} - B_{26}\frac{\partial^3 u_0}{\partial y^3} - B_{16}\frac{\partial^3 v_0}{\partial x^3} - (B_{12}+2B_{66})\frac{\partial^3 v_0}{\partial x^2 \partial y} - 3B_{26}\frac{\partial^3 v_0}{\partial x \partial y^2} - B_{22}\frac{\partial^3 v_0}{\partial y^3} + D_{11}\frac{\partial^4 w_b}{\partial x^4} + 2(D_{12}+2D_{66})\frac{\partial^4 w_b}{\partial x^2 \partial y^2} + 4D_{26}\frac{\partial^4 w_b}{\partial x \partial y^3} + D_{22}\frac{\partial^4 w_b}{\partial y^4} + BS_{11}\frac{\partial^4 w_s}{\partial x^4} + 4(D_{16}+BS_{16})\frac{\partial^4 w_s}{\partial x^3 \partial y} + 2(BS_{12}+2BS_{66})\frac{\partial^4 w_s}{\partial x^2 \partial y^2} + 4BS_{26}\frac{\partial^4 w_s}{\partial x \partial y^3} + BS_{22}\frac{\partial^4 w_s}{\partial y^4} = N_x^T\frac{\partial^2(w_b+w_s)}{\partial x^2} + N_y^T\frac{\partial^2(w_b+w_s)}{\partial y^2} + 2N_{xy}^T\frac{\partial^2(w_b+w_s)}{\partial x \partial y} \quad (26)$$

$$\delta w_s: -AS_{11}\frac{\partial^3 u_0}{\partial x^3} - 3AS_{16}\frac{\partial^3 u_0}{\partial x^2 \partial y} - (AS_{12}+2AS_{66})\frac{\partial^3 u_0}{\partial x \partial y^2} - AS_{26}\frac{\partial^3 u_0}{\partial y^3} - AS_{16}\frac{\partial^3 v_0}{\partial x^3} - (AS_{12}+2AS_{66})\frac{\partial^3 v_0}{\partial x^2 \partial y} - 3AS_{26}\frac{\partial^3 v_0}{\partial x \partial y^2} - AS_{22}\frac{\partial^3 v_0}{\partial y^3} + BS_{11}\frac{\partial^4 w_b}{\partial x^4} + 2(BS_{12}+2BS_{66})\frac{\partial^4 w_b}{\partial x^2 \partial y^2} + 4BS_{16}\frac{\partial^4 w_b}{\partial x^3 \partial y} + 4BS_{26}\frac{\partial^4 w_b}{\partial x \partial y^3} + BS_{22}\frac{\partial^4 w_b}{\partial y^4} + ASS_{11}\frac{\partial^4 w_s}{\partial x^4} + 2(ASS_{12}+2ASS_{66})\frac{\partial^4 w_s}{\partial x^2 \partial y^2} +$$

$$4ASS_{16}\frac{\partial^4 w_s}{\partial x^3 \partial y}+4ASS_{26}\frac{\partial^4 w_s}{\partial x \partial y^3}+ASS_{22}\frac{\partial^4 w_s}{\partial y^4}-2ACC_{45}\frac{\partial^2 w_s}{\partial x \partial y}-ACC_{55}\frac{\partial^2 w_s}{\partial x^2}-ACC_{44}\frac{\partial^2 w_s}{\partial y^2}=$$
$$\mathrm{N_x^T}\frac{\partial^2(\mathrm{w_b}+\mathrm{w_s})}{\partial \mathrm{x}^2}+\mathrm{N_y^T}\frac{\partial^2(\mathrm{w_b}+\mathrm{w_s})}{\partial \mathrm{y}^2}+\ 2\mathrm{N_{xy}^T}\frac{\partial^2(\mathrm{w_b}+\mathrm{w_s})}{\partial \mathrm{x}\,\partial \mathrm{y}} \quad (27)$$

5. NAVIER SOLUTION

The Navier solution is used to analyze laminated composite plates for bending, buckling, and free vibration. cross and angle ply simply supported at all four edgings satisfactorily for the following boundary conditions **(Sayyad, Shinde, and Ghugal, 2016)**

5.1- Navier Solution For cross-ply laminates (SS-1)

Boundary conditions for cross-ply laminate (SS-1) are (Reddy, 2003)

$$at\ x=0\ \ and\ x=a:\ v_0=w_b=w_s=M_x^b=M_x^s=0 \quad (28)$$

$$at\ y=0\ \ and\ y=a:\ u_0=w_b=w_s=M_y^s=M_y^s\ =0 \quad (29)$$

$$u_0(x,y,t)=\sum_{n=1}^{\infty}\sum_{m=1}^{\infty}U_{mn}\ cos\,\alpha x\ sin\,\beta y \quad (30)$$

$$v_0(x,y,t)=\sum_{n=1}^{\infty}\sum_{m=1}^{\infty}V_{mn}\sin\alpha x\ \cos\beta y \quad (31)$$

$$w_b(x,y,t)=\sum_{n=1}^{\infty}\sum_{m=1}^{\infty}W_{bmn}\sin\alpha x\ \sin\beta y \quad (32)$$

$$w_s(x,y,t)=\sum_{n=1}^{\infty}\sum_{m=1}^{\infty}W_{smn}\sin\alpha x\ \sin\beta y \quad (33)$$

5.2- Navier Solution For Angle-ply laminates (SS-2)

Boundary conditions for angle-ply laminate (SS-2) are (Reddy, 2003)

$$at\ x=0\ \ and\ x=a:\ u_0=w_b=w_s=M_x^b=M_x^s\ =0 \quad (34)$$

$$at\ y=0\ \ and\ y=a:\ v_0=w_b=w_s=M_y^s=M_y^s=0 \quad (35)$$

$$u_0(x,y,t)=\sum_{n=1}^{\infty}\sum_{m=1}^{\infty}U_{mn}\ \sin\alpha x\ cos\,\beta y \quad (36)$$

$$v_0(x,y,t)=\sum_{n=1}^{\infty}\sum_{m=1}^{\infty}V_{mn}\cos\alpha x\ \sin\beta y \quad (37)$$

$$w_b(x,y,t)=\sum_{n=1}^{\infty}\sum_{m=1}^{\infty}W_{bmn}\sin\alpha x\ \sin\beta y \quad (38)$$

$$w_s(x,y,t)=\sum_{n=1}^{\infty}\sum_{m=1}^{\infty}W_{smn}\sin\alpha x\ \sin\beta y \quad (39)$$

Where $\alpha=m\,\pi/a$ and $\beta=n\,\pi/b$ and $(U_{mn},V_{mn},W_{bmn},W_{smn})$ are coefficients to be determined

6. THERMAL BUCKLING ANALYSIS

After substituting Navier, s series Eqs (30)-(33) in equations of motion, Eqs (24)-(27), also when substituting Eqs (36)-(39) in Eqs (24)-(27), The values of compressive forces in-plane are taken from Eqs. (13) and (14), the following Eigenvalue problem for cross-ply and angle ply, is obtained:

$$\begin{Bmatrix} K_{11} & K_{12} & K_{13} & K_{14} \\ K_{12} & K_{22} & K_{23} & K_{24} \\ K_{13} & K_{23} & K_{33}-(k_1\alpha^2+k_2\beta^2)\Delta T & K_{34}-(k_1\alpha^2+k_2\beta^2)\Delta T \\ K_{14} & K_{24} & K_{34}-(k_1\alpha^2+k_2\beta^2)\Delta T & K_{44}-(k_1\alpha^2+k_2\beta^2)\Delta T \end{Bmatrix} \begin{Bmatrix} U_{mn} \\ V_{mn} \\ W_{bmn} \\ W_{smn} \end{Bmatrix} = \begin{Bmatrix} 0 \\ 0 \\ 0 \\ 0 \end{Bmatrix} \quad (40)$$

Afterward, for nontrivial solutions, the coefficient matrix's determinant in Eq. (40) must be zero.

7. NUMERICAL RESULTS AND DISCUSSION

Trigonometric displacement function is used in the present work to analyze the critical temperature of the simply supported laminate plate both cross-ply and angle-ply for the first time. In this portion, the effect of changing some design parameters such as orthotropy ratio (E1/E2), aspect ratio (a/b), thickness ratio (a/h), thermal expansion coefficient ratio (α2/α1), are investigated, which have the same behavior and good agreement when compared with previously published results.

7.1 Verification of Results

To verify the derived equations and program built using Matlab, present work results are verified by comparison with the numerical results obtained with different theories used by researchers and give good agreement as shown in the following tables, the discrepancy and the results are very close between the present work with Refined Plate Theory (RPT) that used a different displacement field.

Material 1:

$E_1/E_2=25, G_{12}=G_{13}=0.5E_2, G_{23}=0.2E_2, \nu_{12}=0.25, \alpha_2/\alpha_1=3, E_2=1\ Gpa\ \alpha_{1=10}{}^{-6}\ C^{-1}$

Material 2:

$E_1/E_0=30, E_2/E_0=1, G_{12}=G_{13}=0.65E_0, G_{23}=0.639E_0, \nu_{12}=0.21, \alpha_2/\alpha_0=16, \alpha_1/\alpha_0=-0.21, E_0=10GPa, \alpha_0=10^{-6}$

Material 3:

$E_1/E_0=15, E_2/E_0=1, G_{12}=G_{13}=0.5E_0, G_{23}=0.3356E_0, \nu_{12}=0.3, \alpha_2/\alpha_0=1, \alpha_1/\alpha_0=0.015, E_0=1GPa, \alpha_0=10^{-6}$

Table 1 shows the normalized critical buckling temperature of the symmetric different cross-ply laminated composite square plate with the thickness ratio (a/h) ranging from (4 to 1000) and The dimensionless of critical temperatures was ($Tcr = T * a^2 * h/\pi^2 * D22$) with material properties using (Material 1) (Mansouri and Shariyat, 2014), Observed that the critical buckling temperature increases (the result listed is inversely since it divided by D22) when a number of layers increases for all thickness ratio due to stiffness increases, The results of present work are compared with other theories and give good agreement.

Table 2 and Fig. (1) (a) show a good agreement between present theory results and other theories that study the influence of the thermal expansion coefficients ratio (α2/ α1) on critical temperature for the antisymmetric angle-ply $(45/-45)_3$ laminated plates with the dimensionless ($Tcr = 10^3 *$

$T^*\alpha_0$), thickness ratio (a/h=10) and material properties using (Material 2) **(Mansouri and Shariyat, 2014)**, from which the normalized critical temperature decreases when increasing thermal expansion coefficient ratio due to softening the plates. Also, in **Table 3 and Fig.(1)(b)** effects of different modulus ratio (E1/E2) ranging from (2 to 50) on critical buckling temperature for (6) layers of antisymmetric angle-ply $(45/-45)_3$ plates with thickness ratio (a/h = 10), with the dimensionless ($Tcr = 10^3 * T^*\alpha_0$) and the material properties using (Material 2) **(Mansouri and Shariyat, 2014)** is investigated and noted that when increasing modulus ratio, the normalized critical temperature increase because stiffness increase. **Table 4** displays another comparison with the results of previous theories, the effect of changing in thickness ratio (a/h) ranging from (10/3 to 100) on critical buckling temperatures for antisymmetric (10 layer) angle-ply $(\pm\theta)_5$ laminated plates all edges simply-supported with material properties using (Material 3) **(Mansouri and Shariyat, 2014)** and dimensionless ($Tcr = T^*\alpha_0$), observed that the maximum critical buckling temperature is obtained for the plate with 45^o angle, the results are close to results of previous theories.

7.2 Effect of Design Parameters

The behavior of critical temperature with changing some design parameters is investigated. The critical temperature is decreasing when the thickness ratio (a/h) and Coefficient of Thermal Expansion (CTE) ratio increased and it increases when the number of plies and orthotropy ratio is increased for angle ply laminated plates while maximum thermal buckling temperature is obtained for the plate with 45^o angle, as shown in the following tables below this behavior is caused by stiffness differences.

7.2.1 Antisymmetric and Symmetric Cross-ply of the simply supported various composite laminate thick and thin plate

For this type, the dimensionless ($Tcr = T^*a^2*h/\pi^2 * D_{22}$) and material properties using (Material1) (the results listed of (a/h) ratio is inversely since it divided by D22).

Table 5 displays the influence of changing of thickness ratio (a/h) and aspect ratio (a/b) on critical buckling temperatures of laminate plate $[(0/90)_S,(0/90)_3]$. The results show that critical buckling temperatures increase when the aspect ratio (a/b) increases along with the thickness ratio (a/h). **Table 6** shows the effect of thermal expansion coefficient ratio ($\alpha2/\alpha1$) on critical buckling temperature for different thickness ratio (a/h) of laminate plate $[(0/90)_S,(0/90)_3]$ as expected, the critical buckling temperature decrease when ($\alpha_2/\ \alpha_1$) increase along (a/h) ratio, there is inversely proportional between the critical buckling temperature parameter and ($\alpha2/\alpha1$) due to thermal buckling strength decrease of the plate when increasing $\alpha2$. Effect of changing orthotropy ratio (E1/E2) on critical buckling temperature for antisymmetric $[(0/90),(0/90)_2, (0/90)_4]$ plates are listed in **Table 7** with varied thickness ratio (a/h), the results are clear that the nondimensionalized buckling load decreases for antisymmetric laminates as the modulus ratio (E1/E2) increases.

7.2.2 Antisymmetric angle-ply of the simply supported various composite laminate plate

For this type, the dimensionless ($Tcr = T^* \alpha_0$) and material properties given by (Material 3).

The effect of changing of thickness ratio (a/h) and aspect ratio (a/b) on critical buckling temperatures of antisymmetric [(45/-45)2,(45/-45)3] laminate plate is listed in **Table 8**. The results show that critical buckling temperatures increase when aspect ratio (a/b) increase. **Table 9** shows the effect of thermal expansion coefficient ratio (α_2/α_1) on critical buckling temperature for different thickness ratio (a/h) of antisymmetric [(45/-45)2,(45/-45)3] laminate plate the critical buckling temperature decreases when both (α_2/α_1) and (a/h) increase, There is an inverse relationship between the critical buckling temperature parameter and ($\alpha 2/\alpha 1$) due to the plate's thermal buckling strength decreasing as $\alpha 2$ increasing. Finally, **Table 10** illustrates the effect of changing moduli ratio (E_1/E_2) on critical buckling temperature of antisymmetric [(45/-45)2,(45/-45)4] for different thickness ratios (a/h) observed when (E_1/E_2) increase the critical buckling temperatures increasing, but it decrease when (a/h) increase. Different critical thermal buckling modes for plates with different aspect ratios for cross and angle square plates are shown in **Fig.2**.

Table 1.Normalized critical temperature for different thickness ratios (a/h) square plate with symmetrical cross-ply

Lay-up	a/h	TOST	RPT	Present work	Discrepancy %
$(0/90)_S$	4	0.0575	0.07115	0.07155	0.5%
	10	0.1522	0.17492	0.1750	0.05%
	100	0.2435	0.24405	0.2440	0.02%
	1000	0.2450	0.24510	0.2450	0.04%
$(0/90)_{2S}$	4	0.0315	0.03348	0.03367	0.5%
	10	0.0797	0.08231	0.08237	0.07%
	100	0.1148	0.11485	0.11484	$8.7*10^{-3}$%
	1000	0.1153	0.11530	0.1153	0
$(0/90)_{5S}$	4	0.0247	0.02541	0.02555	0.55%
	10	0.0621	0.06247	0.06251	0.064%
	100	0.0872	0.08716	0.08716	0
	1000	0.0875	0.08759	0.08750	0.15

Table 2. Normalized critical temperature for the simply supported antisymmetric $(\pm 45)_3$ angle-ply square plates.

$\alpha 2/\ \alpha 1$	LWT	TOST	RPT	Preset work	Discrepancy %	DQ results GRT (9×9)		
						P=3(TOT)	P=5	P=7
1	9.3134	10.3868	10.3854	10.3877	0.02%	10.3867	10.4707	10.5638
5	8.0703	9.0003	8.9991	9.0011	0.02%	9.0003	9.0730	9.1537
10	6.9163	7.7134	7.7123	7.7140	0.02%	7.7133	7.7757	7.8448
20	5.3782	5.9980	5.9972	5.9985	0.02%	5.9980	6.0465	6.1002
30	4.3998	4.9068	4.9062	4.9072	0.02%	4.9068	4.9464	4.9904
40	3.7225	4.1515	4.1510	4.1519	0.019%	4.1515	4.1851	4.2223
50	3.2260	3.5978	3.5973	3.5980	0.019%	3.5977	3.6268	3.6591

Table 3. Normalized (ΔT_{Cr}) for different orthotropy ratios (E1/E2) for antisymmetric $(\pm 45)_3$ square plates.

E1/E2	LWT	TOST	RPT (13×13)	Present work	Discrepancy %	DQ results GRT (9×9)		
						P=3 (TOST)	P=5	P=7
2	2.4672	2.4721	2.4721	2.4722	4*10-3%	2.4721	2.4744	2.4771
5	4.6703	4.7728	4.7728	4.7730	4.1*10-3%	4.7728	4.7823	4.7928
10	8.1229	8.5390	8.5386	8.5391	5.8*10-3%	8.5390	8.5697	8.6029
15	11.5069	12.3517	12.3509	12.3518	7.2*10-3%	12.3517	12.413	12.4799
20	14.9536	16.3091	16.3079	16.3094	9.1*10-3%	16.3090	16.409	16.5195
30	22.4823	25.0733	25.0700	25.0756	0.022%	25.0733	25.2756	25.5007
40	31.7113	35.9042	35.8980	35.9117	0.038%	35.9041	36.2438	36.6308
50	44.2904	50.6840	50.6737	50.7028	0.057%	50.6840	51.2138	51.8351

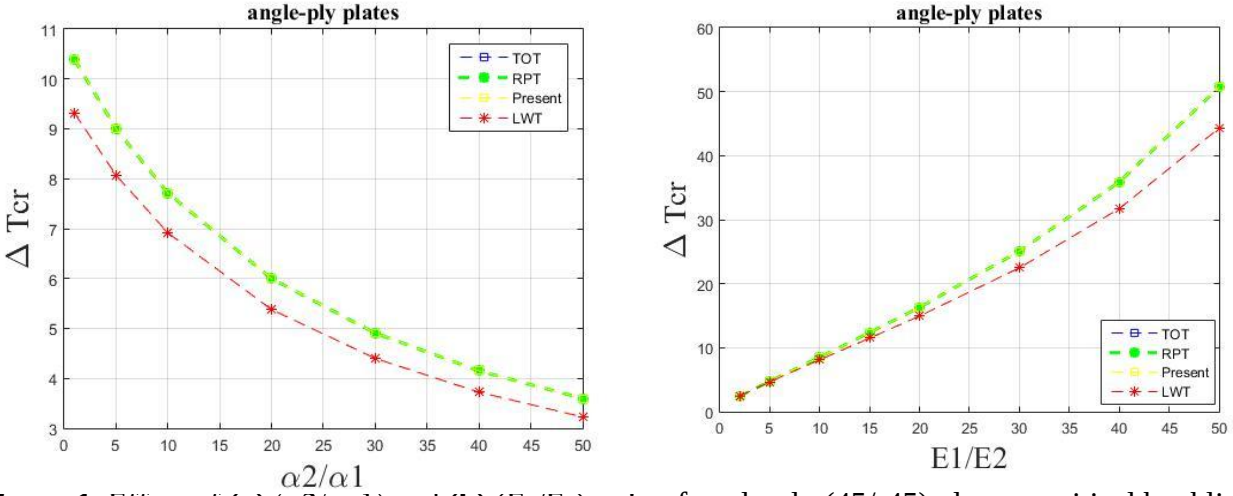

Figure 1. Effect of **(a)** ($\alpha 2/\ \alpha 1$) and **(b)** (E_1/E_2) ratio of angle-ply (45/-45) plate on critical buckling temperature ΔT_{cr}

Table 4. Normalized critical temperature for the simply supported antisymmetric $(\pm\theta)_5$ angle-ply square plates.

a/h	Θ	3D	TOST	GHOT	RPT	Present	Discrepancy %	GRT P=7
100	0	$7.463*10^{-4}$	$7.470*10^{-4}$	$7.463*10^{-4}$	$7.470*10^{-4}$	$7.469*10^{-4}$	0.013%	$7.466*10^{-4}$
	15	$1.115*10^{-3}$	$1.116*10^{-3}$	$1.115*10^{-3}$	$1.116*10^{-3}$	$1.1159*10^{-3}$	$8.9*10^{-3}$%	$1.115*10^{-3}$
	30	$1.502*10^{-3}$	$1.502*10^{-3}$	$1.502*10^{-3}$	$1.502*10^{-3}$	$1.502*10^{-3}$	0	$1.502*10^{-3}$
	45	$1.674*10^{-3}$	$1.675*10^{-3}$	$1.675*10^{-3}$	$1.675*10^{-3}$	$1.675*10^{-3}$	0	$1.675*10^{-3}$
20	0	$1.739*10^{-2}$	-	$1.739*10^{-2}$	$1.772*10^{-2}$	$1.773*10^{-2}$	0.056%	$1.757*10^{-2}$
	15	$2.528*10^{-2}$	-	$2.531*10^{-2}$	$2.591*10^{-2}$	$2.590*10^{-2}$	0.038%	$2.562*10^{-2}$
	30	$3.446*10^{-2}$	-	$3.456*10^{-2}$	$3.477*10^{-2}$	$3.477*10^{-2}$	0	$3.484*10^{-2}$

	45	$3.810*10^{-2}$	-	$3.826*10^{-2}$	$3.844*10^{-2}$	$3.844*10^{-2}$	0	$3.859*10^{-2}$
10	0	$5.782*10^{-2}$	$5.778*10^{-2}$	$5.782*10^{-2}$	$6.125*10^{-2}$	$6.127*10^{-2}$	0.032%	$5.963*10^{-2}$
	15	$7.904*10^{-2}$	$7.920*10^{-2}$	$7.933*10^{-2}$	$8.478*10^{-2}$	$8.481*10^{-2}$	0.035%	$8.211*10^{-2}$
	30	0.1100	0.1108	0.1110	0.1130	0.1130	0	0.1137
	45	0.1194	0.1208	0.1209	0.1225	0.1225	0	0.1240
$\frac{20}{3}$	0	0.1029	-	0.1029	0.1124	0.1125	0.088%	0.1081
	15	0.1322	-	0.1330	0.1466	0.1468	0.13%	0.1399
	30	0.1859	-	0.1888	0.1940	0.1942	0.1%	0.1958
	45	0.1981	-	0.2023	0.2062	0.2065	0.14%	0.2101
5	0	0.1436	0.1417	0.1436	0.1591	0.1593	0.125%	0.1524
	15	0.1753	0.1746	0.1765	0.1975	0.1979	0.2%	0.1874
	30	0.2377	0.2421	0.2432	0.2597	0.2604	0.26%	0.2575
	45	-	0.2651	0.2656	0.2720	0.2728	0.29%	0.2777
4	0	0.1777	-	0.1777	0.1974	0.1980	0.3%	0.1893
	15	0.2087	-	0.2103	0.2360	0.2370	0.42%	0.2239
	30	-	-	0.2754	0.3091	0.3105	0.45%	0.2922
	45	-	-	0.3114	0.3204	0.32211	0.5%	0.3266
$\frac{10}{3}$	0	0.2057	-	0.2057	0.2277	0.2287	0.43%	0.2190
	15	0.2347	-	0.2367	0.2651	0.2668	1%	0.2518
	30	-	-	0.2988	0.3376	0.3413	1%	0.3170
	45	-	-	0.3443	0.3564	0.3592	0. 49%	0.3614

Table 5. Normalized critical temperature for various aspect ratios (a/b) for symmetric and antisymmetric.

layup	a/b	ΔT_{cr}				
		a/h				
		4	5	10	20	100
$(0/90)_S$	1	0.07155	0.09528	0.1750	0.2226	0.2440
	2	0.07620	0.1039	0.2118	0.2894	0.3282
	3	0.08593	0.1218	0.3027	0.4965	0.6267
	4	0.09459	0.1357	0.3808	0.7430	1.077
$(0/90)_3$	1	0.02117	0.02810	0.0509	0.0642	0.0701
	2	0.02834	0.04022	0.10244	0.1738	0.2248
	3	0.03416	0.0482	0.1404	0.3106	0.5205
	4	0.04066	0.05555	0.1634	0.4230	0.9287

Table 6. Normalized critical temperature for different (α_2/α_1) for symmetric and antisymmetric

layup	α2/ α1	Tcr				
		a/h				
		4	5	10	20	100
(0/90)s	4	0.0686	0.09134	0.16781	0.2134	0.2339
	6	0.06336	0.08437	0.1550	0.1971	0.2161
	8	0.05887	0.07838	0.1440	0.1831	0.2007
	10	0.05497	0.07319	0.1344	0.1710	0.1874
$(0/90)_3$	4	0.0203	0.02694	0.04884	0.06159	0.06724
	6	0.01875	0.02489	0.04511	0.05689	0.06211
	8	0.01742	0.02312	0.04191	0.05286	0.05770
	10	0.01626	0.02159	0.03913	0.04935	0.05388

Table 7. Normalized critical temperature for different (E1/E2) antisymmetric square plates .

layup	a/h	Tcr				
		E1/E2				
		10	15	25	30	40
(0/90)	4	0.06117	0.03462	0.01644	0.01254	0.008146
	10	0.09025	0.05294	0.02680	0.02103	0.01439
	20	0.09693	0.05736	0.02952	0.02336	0.01623
	100	0.09929	0.05894	0.03052	0.02422	0.01693
$(0/90)_2$	4	0.07456	0.04307	0.0202	0.01517	0.009518
	10	0.1321	0.08543	0.0473	0.03785	0.02625
	20	0.1488	0.09971	0.05891	0.04855	0.03555
	100	0.1551	0.1053	0.06395	0.05341	0.04013
$(0/90)_4$	4	0.07865	0.04573	0.02153	0.01618	0.01016
	10	0.1426	0.09344	0.05222	0.04183	0.02902
	20	0.1618	0.1102	0.06611	0.05469	0.04021
	100	0.1690	0.1169	0.07230	0.0607	0.04592

Table 8. Normalized (ΔTcr) for different aspect ratio (a/b) antisymmetric (45/-45) angle-ply plates.

layup	a/b	Tcr			
		a/h			
		4	10	20	100
(45/-45)2	1	0.3004	0.1101	0.03396	0.001468
	2	0.3727	0.1830	0.06653	0.003119
	3	0.4205	0.2438	0.1037	0.005372
	4	0.4622	0.2932	0.1435	0.008374
$(45/-45)_3$	1	0.3144	0.1183	0.03692	0.001605
	2	0.2447	0.07181	0.02042	0.000854
	3	0.2146	0.05726	0.01584	0.000656
	4	0.2004	0.05126	0.01402	0.000578

Table 9. Normalized critical temperature for simply supported square plate for different (α_2/α_1)

layup	α2/ α1	Tcr			
		a/h			
		4	10	20	100
$(45/-45)_2$	4	0.02241	0.008216	0.002533	0.000109
	6	0.01989	0.007291	0.002248	0.0000972
	8	0.01787	0.006553	0.002021	0.0000874
	10	0.01623	0.005951	0.001835	0.0000793
$(45/-45)_3$	4	0.02346	0.008828	0.002755	0.0001197
	6	0.02081	0.007835	0.002444	0.0001062
	8	0.01871	0.007042	0.002197	0.0000955
	10	0.01699	0.006395	0.001995	0.0000867

Table 10. Normalized critical temperature for antisymmetric angle-ply square plates for different (E1/E2)

layup	a/h	Tcr				
		E1/E2				
		10	15	25	30	40
$(45/-45)_2$	4	0.2767	0.3004	0.3142	0.3139	0.3077
	10	0.08794	0.1101	0.1389	0.1481	0.1598
	20	0.02567	0.03396	0.0471	0.05231	0.06066
	100	0.00108	0.001468	0.00212	0.00241	0.00291
$(45/-45)_4$	4	0.2933	0.3196	0.3351	0.3350	0.3288
	10	0.09598	0.1212	0.1533	0.1633	0.1757
	20	0.02831	0.0379	0.05317	0.0591	0.0686
	100	0.00120	0.00165	0.00243	0.1633	0.00335

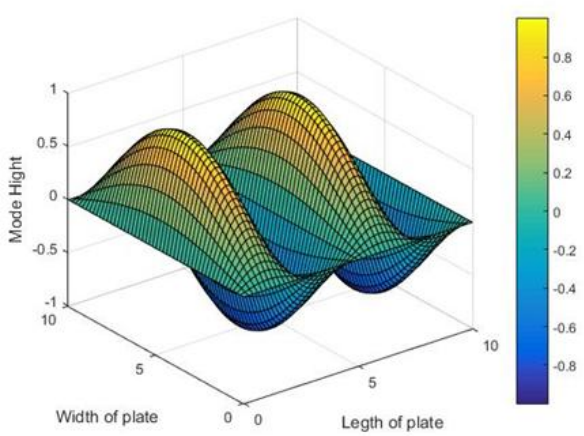

(a) mode (m=4,n=1), No. of layers=4, a/h=10

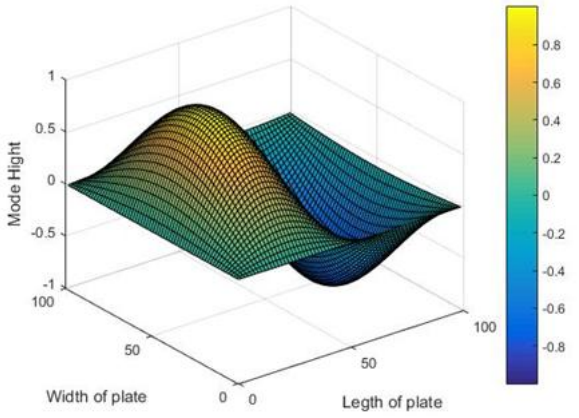

(b) mode (m=2,n=1), No. of layers=8, a/h=100

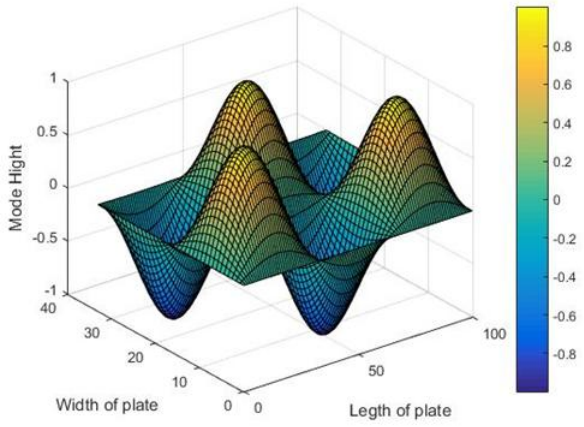

(c) mode (m=3,n=2), No. of layers=4, a/h=100 , b=a/3

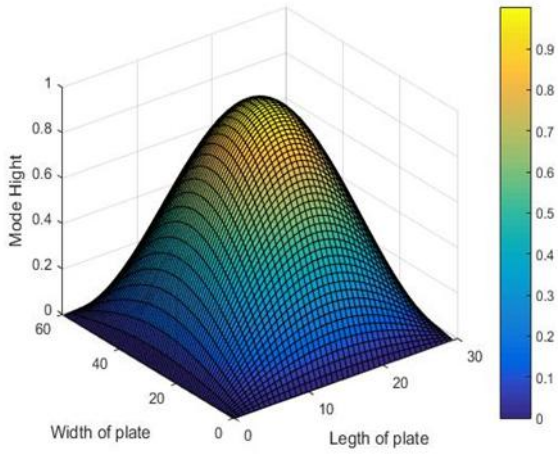

(d) mode (m=1,n=1), No. of layers=4, a/h=30 , a=b/2

Figure 2. Normalized Thermal Buckling mode for antisymmetric angle-ply and cross-ply plate.

8. CONCLUSIONS

The thermal buckling behaviors of laminate plates have been described and discussed in this work by using a simple trigonometric shear deformation theory. The most significant characteristic of this theory is that it contains only four unknowns, as opposed to five in first-order shear deformation theory and other higher-order theories. Following the above discussions, the preliminary results are summarized as follows:

1- Design parameters as (modulus ratio, aspect ratio, thickness ratio, ($\alpha 2/\alpha 1$) ratio), in addition to the number of layers, have the same behavior that obtained by other different plate theories.

2- The angle ply gives higher critical temperature buckling than cross-ply for the same materials because of stiffness differences

3- Results obtained from present work agree well with other RPT that use different displacement fields for both thick and thin plates also with HSDPT for thin plate,s while discrepancy increased for thick plates.

4- The critical thermal buckling is increased for symmetric and antisymmetric laminates angle-ply when the modulus ratio increases while it decreases for antisymmetric laminates cross-ply.

9. REFERENCES

- Al-Waily, M., Al-Shammari, M. A. and Jweeg, M. J., 2020. An analytical investigation of thermal buckling behavior of composite plates reinforced by carbon nano particles, Journal of *Engineering*, 24(3), pp. 11–21. DOI: 10.4186/ej.2020.24.3.11.
- Cetkovic, M., 2016. Thermal buckling of laminated composite plates using layerwise displacement model, *Composite Structures*, 142, pp. 238–253. DOI: 10.1016/j.compstruct.2016.01.082.
- Do, V. N. Van and Lee, C. H., (2019. Mesh-free thermal buckling analysis of multilayered composite plates based on an nth-order shear deformation theory, *Composite Structures*, 224(April), p. 111042. DOI: 10.1016/j.compstruct.2019.111042.
- Hussein, E. Q. and Alasadi, S. J., 2018. Experimental and Theoretical Stress Analysis Investigation for Composite Plate Under Thermal Load, pp. 205–221.
- Jameel, A. N., Sadiq, I. A. and Nsaif, Hasanain, I., 2012. Buckling Analysis of Composite Plates under Thermal and Mechanical Loading, *Journal of Engineering*, 18, November, pp. 1365–90.
- Jin, T. *et al.*, 2015. Thermal buckling measurement of a laminated composite plate under a uniform temperature distribution using the digital image correlation method, *Composite Structures*, 123, pp. 420–429. DOI: 10.1016/j.compstruct.2014.12.025.
- Kiani, Y., 2020. NURBS-based thermal buckling analysis of graphene platelet reinforced composite laminated skew plates, *Journal of Thermal Stresses*, 43(1), pp. 90–108. DOI: 10.1080/01495739.2019.1673687.
- Manickam, G. *et al.*, 2018. Thermal buckling behaviour of variable stiffness laminated

composite plates, *Materials Today Communications*, 16, pp. 142–151. DOI: 10.1016/j.mtcomm.2018.05.003.

- Mansouri, M. H., and Shariyat, M., 2014. Thermal buckling predictions of three types of high-order theories for the heterogeneous orthotropic plates, using the new version of DQM, *Composite Structures*, 113(1), pp. 40–55. DOI: 10.1016/j.compstruct.2014.02.032.
- Ounis, H., Tati, A. and Benchabane, A., 2014. Thermal buckling behavior of laminated composite plates: A finite-element study, *Frontiers of Mechanical Engineering*, 9(1), pp. 41–49. DOI: 10.1007/s11465-014-0284-z.
- Reddy, J. N., 2003. Mechanics of Laminated Composite Plates and Shells, *Mechanics of Laminated Composite Plates and Shells*. DOI: 10.1201/b12409.
- Sadiq, I. A., and Majeed, W., 2019. Thermal Buckling of Angle-Ply Laminated Plates Using New Displacement Function, *Journal of Engineering*, 25(12), pp. 96–113. DOI: 10.31026/j.eng.2019.12.08.
- Sayyad, A. S., Shinde, B. M., and Ghugal, Y. M., 2016. Bending, vibration and buckling of laminated composite plates using a simple four variable plate theory, *Latin American Journal of Solids and Structures*, 13(3), pp. 516–535. DOI: 10.1590/1679-78252241.
- Shaterzadeh, A. R., Abolghasemi, S., and Rezaei, R., 2014. Finite element analysis of thermal buckling of rectangular laminated composite plates with circular cut-out, *Journal of Thermal Stresses*, 37(5), pp. 604–623. DOI: 10.1080/01495739.2014.885322.
- Shen, H. S., 2013. Thermal buckling and postbuckling of functionally graded fiber-reinforced composite laminated plates, *Journal of Composite Materials*, 47(22), pp. 2783–2795. DOI: 10.1177/0021998312458131.
- Tocci Monaco, G. *et al.*, 2020. Hygro-thermal vibrations and buckling of laminated nanoplates via nonlocal strain gradient theory, *Composite Structures*, p. 113337. DOI: 10.1016/j.compstruct.2020.113337.
- Torabi, J., Ansari, R., and Hassani, R., 2019. Numerical study on the thermal buckling analysis of CNT-reinforced composite plates with different shapes based on the higher-order shear deformation theory, *European Journal of Mechanics, A/Solids*, 73(May 2018), pp. 144–160. DOI: 10.1016/j.euromechsol.2018.07.009.
- Tran, L. V., Wahab, M. A. and Kim, S. E., 2017. An isogeometric finite element approach for thermal bending and buckling analyses of laminated composite plates., *Composite Structures*, 179, pp. 35–49. DOI: 10.1016/j.compstruct.2017.07.056.
- Vescovini, R. *et al.*, 2017. Thermal buckling response of laminated and sandwich plates using refined 2-D models, *Composite Structures*, 176, pp. 313–328. DOI: 10.1016/j.compstruct.2017.05.021.
- Vosoughi, A. R. and Nikoo, M. R., 2015. Maximum fundamental frequency and thermal buckling temperature of laminated composite plates by a new hybrid multi-objective optimization technique, *Thin-Walled Structures*, 95, pp. 408–415. DOI: 10.1016/j.tws.2015.07.014.
- Xing, Y., and Wang, Z., 2017. Closed form solutions for thermal buckling of functionally graded rectangular thin plates, *Applied Sciences (Switzerland)*, 7(12). DOI:

10.3390/app7121256.

- Yang, X. *et al.*, 2020. Thermal buckling and dynamic characteristics of composite plates under pressure load, *Journal of Mechanical Science and Technology*, 34(8), pp. 3117–3125. DOI: 10.1007/s12206-020-0702-6.

APPENDIX

Where the matrix elements of the stiffness.K_{ij} in cross-ply laminate are:

$$K_{11} = (A_{11}\alpha^2 + A_{66}\beta^2) \quad , \quad K_{12} = (A_{12} + A_{66})\alpha\beta$$

$$K_{13} = -(B_{11}\alpha^3 + (B_{12} + 2B_{66})\alpha\beta^2) \quad , \quad K_{14} = -(AS_{11}\alpha^3 + (AS_{12} + 2AS_{66})\alpha\beta^2)$$

$$K_{22} = (A_{66}\alpha^2 + A_{22}\beta^2) \quad , \quad K_{23} = -(B_{22}\beta^3 + (B_{12} + 2B_{66})\alpha^2\beta)$$

$$K_{24} = -(AS_{22}\beta^3 + (AS_{12} + 2AS_{66})\alpha^2\beta)$$

$$K_{33} = (D_{11}\alpha^4 + 2(D_{12} + 2D_{66})\alpha^2\beta^2 + D_{22}\beta^4)$$

$$K_{34} = (BS_{11}\alpha^4 + 2(BS_{12} + 2BS_{66})\alpha^2\beta^2 + BS_{22}\beta^4)$$

$$K_{44} = (ASS_{11}\alpha^4 + 2(ASS_{12} + 2ASS_{66})\alpha^2\beta^2 + ASS_{22}\beta^4 + ACC_{55}\alpha^2 + ACC_{44}\beta^2)$$

$$A_{16} = A_{26} = B_{16} = B_{26} = D_{16} = D_{26} = AS_{16} = AS_{26} = BS_{16} = BS_{26} = ASS_{16} = ASS_{26} = ACC_{45} = 0$$

And the element of the stiffness matrix K_{ij} in angle-ply laminate are:

$$K_{11} = (A_{11}\alpha^2 + A_{66}\beta^2) \quad , \quad K_{12} = (A_{12} + A_{66})\alpha\beta$$

$$K_{13} = -(3B_{16}\alpha^2\beta + B_{26}\beta^3) \quad , \quad K_{14} = -(3AS_{16}\alpha^2\beta + AS_{26}\beta^3)$$

$$K_{22} = (A_{66}\alpha^2 + A_{22}\beta^2) \quad , \quad K_{23} = -(B_{16}\alpha^3 + 3B_{26}\,\alpha\beta^2)$$

$$K_{24} = -(AS_{16}\alpha^3 + 3AS_{26}\,\alpha\beta^2)$$

$$K_{33} = (D_{11}\alpha^4 + 2(D_{12} + 2D_{66})\alpha^2\beta^2 + D_{22}\beta^4)$$

$$K_{34} = (BS_{11}\alpha^4 + 2(BS_{12} + 2BS_{66})\alpha^2\beta^2 + BS_{22}\beta^4)$$

$$K_{44} = (ASS_{11}\alpha^4 + 2(ASS_{12} + 2ASS_{66})\alpha^2\beta^2 + ASS_{22}\beta^4 + ACC_{55}\alpha^2 + ACC_{44}\beta^2)$$

$$A_{16} = A_{26} = B_{11} = B_{12} = B_{22} = B_{66} = D_{16} = D_{26} = AS_{11} = AS_{12} = AS_{22} = AS_{66} = BS_{16} = BS_{26} = ASS_{16} = ASS_{26} = ACC_{45} = 0$$

The plane stress reduced stiffness Q_{ij} **(Reddy, 2003)** is:

$$Q_{11} = \frac{E_1}{1 - v_{12}v_{21}}, \quad Q_{12} = \frac{v_{12}E_2}{1 - v_{12}v_{21}}, Q_{22} = \frac{E_2}{1 - v_{12}v_{21}}, Q_{66} = G_{12}$$

$$Q_{44} = G_{23} \ , \ Q_{55} = G_{13}$$